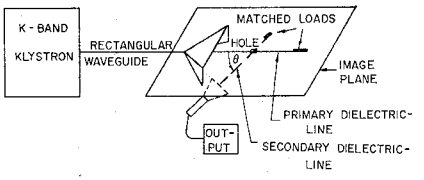

Fig. 2—Experimental set-up.

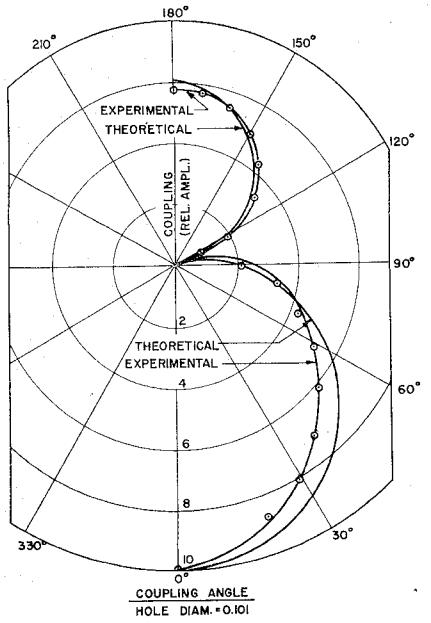

Fig. 3—Coupling as a function of angle θ.

hole acting as a waveguide beyond cut-off. E_n is the normal component of the electric field and H_t is the transverse component of the magnetic field both in the dielectric guide at the coupling hole. The longitudinal component of the magnetic field H_z is neglected. S is a power normalizing factor, h is the diameter of the hole, λ_0 is the free-space wavelength, and η is the specific impedance of free space. Fig. 2 defines the angle θ. If t, the thickness of the plane, is very small, the ratio $F_e(t)/F_H(t) \sim 1$ and the equations further simplify

$$C = T[1 + g \cos \theta]$$

and

$$D = \frac{1 + g \cos \theta}{1 - g \cos \theta}.$$

C and D are given in relative values, T is a constant of proportionality, and g is approximately the ratio of magnetic to electric coupling.

An experimental dielectric image line coupler was investigated at 24.4 kmcps. Fig. 2 illustrates the arrangement of the experiment. The ground plane thickness was 0.026 inch and the hole size was 0.101 inch in diameter. For these dimensions, $F_H(t)$ was 1.112 and $F_e(t)$ was 0.827. The ratio $F_e(t)/F_H(t)$ then is 0.742 and should be used (instead of 1.00) if greater accuracy is called for. Fig. 3 shows the variation of the coupling as a function of the angle θ. Plotted in the same figure is a curve called "Theoretical" which is of the form: $C = T(1 + g \cos \theta)$. The factor g is approximately equal to 4, the ratio of magnetic to electric coupling. The magnitude of the coupling is normalized so that at $\theta = 0°$, $C = 10$. Similar data were taken for hole diameters of 0.078, 0.082, 0.093, 0.111, 0.128 inch with no substantial differences apparent.

Fig. 4 illustrates how this arrangement may be used as a directional coupler. The

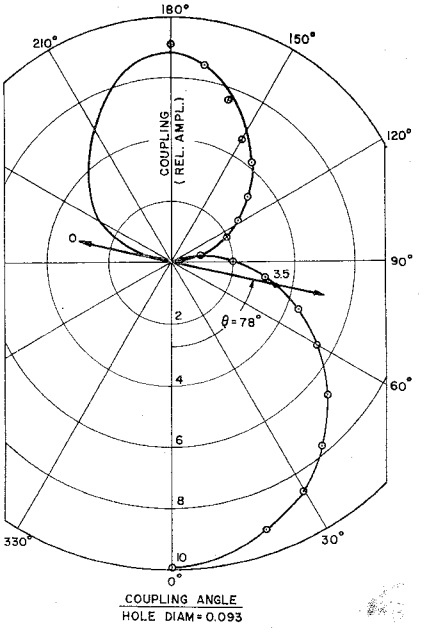

Fig. 4—Direct coupling.

solid line at $\theta = 78°$ represents the orientation of the secondary guide with respect to the primary guide. In one direction, the coupling is approximately zero whereas in the other direction it is 3.5 relative units.

Many other possible arrangements of holes and slots may be used to produce equivalent results or to improve the coupling and directivity behavior.

D. J. Angelakos
Elec. Engrg. Dept.
Univ. of Calif.
Berkeley 4, Calif.

An Extension of the Concept of Stop and Pass Bands of a Zobel Type Filter to a General Reciprocal Two Port Network Which has a Non-loxodromic Transformation*

The conventional treatment[1] of the Zobel filter starts with symmetrical T or π sections of pure reactances and then develops the iterative measures of the network; the fixed points and the propagation constant. It is shown that the propagation constant is either pure real (stop band)[2] or pure imaginary (pass band). These iterative measures can be worked out for the general T section. Fig. 1 shows the nomenclature used for the symmetrical T section and the general two port.

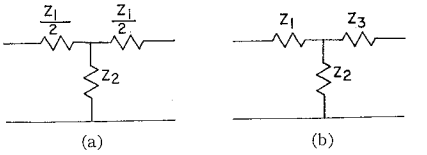

Fig. 1—(a) The symmetrical T section, (b) the asymmetrical T section.

TABLE I

(a) The symmetrical T section

$$\cosh \gamma = 1 + \frac{Z_1}{2Z_2}$$

$$Z_{it} = Z_0 = \pm \sqrt{Z_1 Z_2 + \frac{Z_1^2}{4}}$$

(b) The asymmetrical T section

$$\cosh \gamma = 1 + \frac{Z_1 + Z_3}{2Z_2}$$

$$Z_{it} = Z_1 - Z_3 \pm \sqrt{\left(\frac{Z_1 + Z_3}{2}\right)^2 + (Z_1 + Z_3)Z_2}$$

Table 1 lists the equations for the fixed points and the propagation constant for both networks. The network properties can also be developed as a bilinear transformation,[3] and the network can be classified by its type of transformation. For the two port, the input impedance is related to the output impedance by

$$Z' = \frac{\dfrac{(Z_1+Z_2)Z}{Z_2} + \dfrac{Z_1Z_2+Z_2Z_3+Z_3Z_1}{Z_2}}{\dfrac{1}{Z_2}Z + \dfrac{Z_2+Z_3}{Z_2}}.$$

The trace of the normalized transformation is $2+(Z_1+Z_3)/Z_2$ which is twice cosh γ. For the transformation to be nonloxodromic the trace must be real, hence the sum of the two series impedance phasors is either in phase or 180° out of phase with the phasor impedance of the shunt arm. It has been shown[4] that it is always possible in a microwave two port, to find reference planes at which the transformation is nonloxodromic. Thusly for any microwave network, reference planes can be found where cosh γ is real. If the transformation is hyperbolic ($|a+d| > 2$)γ will be real. If the transformation is elliptic ($|a+d| < 2$)γ will be imagi-

* Received by the PGMTT, March 9, 1959.

[1] W. L. Everitt and G. E. Anner, "Communication Engineering," McGraw-Hill Book Co., Inc., New York, N. Y.; 1956.

[2] With the exception of a possible 180° phase reversal.

[3] E. F. Bolinder, "Impedance and polarization-ratio transformations by a graphical method using isometric circles," IRE Trans. on Microwave Theory and Techniques, vol. MTT-4, pp. 176–180; July, 1956.

[4] D. J. R. Stock and L. J. Kaplan, "The analogy between the Weissfloch transformer and the ideal attenuator (reflection coefficient transformer) and an extension to include the general lossy two port," IRE Trans. on Microwave Theory and Techniques, to be published.

nary and $a+d=\pm 2$ the cut off conditions will be obtained. The cut off may be either between loss and phase shift as in a Zobel filter or between gain and phase shift because the cosine is an even function; therefore, it cannot perceive if the hyperbolic transformation is due to gain (negative resistance) or loss.

If the impedance plane is mapped onto the Riemann sphere, the criterion for determining whether the network is in the stop or pass band will depend on whether the Pascal line[5] cuts or does not cut the Riemann sphere (the parabolic transformation occurs at tangency). These transformation characteristics have been used by Bolinder[6] to show the analogy of the exponential line to the high pass filter and can be used to denote the difference between lossy and lossless uniform transmission lines. This classification can be used for any device, as waveguide, which has cut off phenomena or accounts for losses in any transmission device.

Thus it is seen that it is always possible to find reference terminals for a given network at which the resultant is either pure gain or pure loss or pure phase shift in the Zobel sense. Of course the insertion loss will depend on the termination as well as the properties of the two port.

D. J. R. Stock
L. J. Kaplan
Elec. Engrg. Dept.
New York Univ., N. Y.

[5] E. F. Bolinder, "Impedance transformations by extension of the isometric circle method to the three dimensional hyperbolic space," *J. Math. Phys.*, vol. 36, pp. 49–61; April, 1957.
[6] E. F. Bolinder, "Study of the exponential line by the isometric circle method and hyperbolic geometry," *Acta Pol.*, Elec. Engrg. Series, vol. 7, no. 8; 1957.

Characteristic Impedance of Split Coaxial Line*

A few years ago, the balun was studied at our laboratory and it is important to know the characteristic impedances of the line. There are several papers[1–3] concerning this characteristic impedance. The cross section of the transmission lines is shown in Fig. 1 and the characteristic impedances are calculated in these papers. Last year, a paper was published in the IRE Trans. on Microwave Theory and Technique on this problem, using similar methods described below. I wish to describe my approach and show a disparity.

* Received by the PGMTT, December 9, 1958.
[1] H. Kogō and K. Morita, "Electrode capacity of slit-coaxial cylinder," *J. Inst. Elec. Commun. Eng., Japan*, vol. 38, pp. 548–552; July, 1955.
[2] H. Kogō and K. Morita, "Electrode capacity of slit-coaxial cylinder," (supplement) *J. Inst. Elec. Commun. Eng., Japan*, vol. 39, pp. 33–36; January, 1956.
[3] J. Smolarska, "Characteristic impedance of the slotted coaxial line," IRE Trans. on Microwave Theory and Techniques, vol. MTT-6, pp. 161–164; April, 1958.

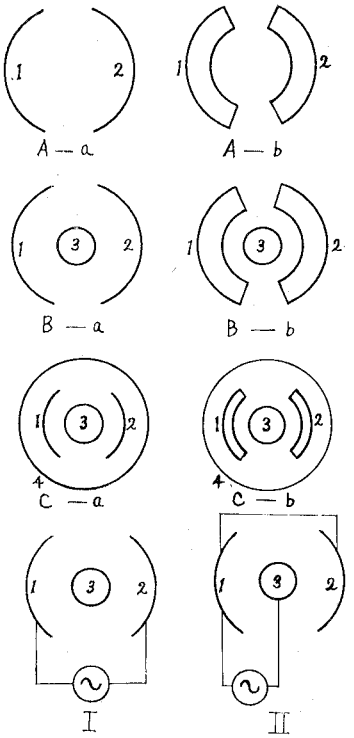

Fig. 1—Cross section of the transmission lines and line construction. A) Split cylinder, B) split coaxial, C) split coaxial with outer pipe; a) thin outer wall, b) thick outer wall; I) line composed of sides 1, 2, II) line composed of sides 1, 2 and central conductor 3.

The characteristic impedance of the split coaxial line shown in Fig. 1 can be classified physically and mathematically as follows:

A) The split cylinder
  a) the thin outer wall
  b) the thick outer wall
B) The split coaxial line
  a) the thin outer wall
  b) the thick outer wall
C) The split coaxial with outer pipe.

There are two cases. In the first case, the split two sides 1 and 2, compose the transmission line (I) and, in the second case, the split two side 1 and 2, and a central conductor 3 form the transmission line (II) shown in Fig. 1. The mathematical treatment of these cases are difficult because of the thickness of the outer conductors, *A-a*, *A-b*, and *B-a* in the above table are described in a previous treatise.[1,2] The same results were obtained by J. Smolarska by using a similar method. For the remaining problems *B-b*, one must rely on an approximate solution, the accurate solution being much too difficult.

The characteristic impedance of *B-b* with regard to the split coaxial shown in Fig. 2, is acquired from the accurate solution by using the accurate values of the characteristic impedances of the split cylinder considering wall thickness and the split coaxial with thin outer wall.

The characteristic impedance composed of the outer and a central conductor of *B-b* is almost equal to that compared with the case of a zero thickness since the width of the split is narrow and the disturbance of the split portion shown in Fig. 3 differs slightly by the existence of the thickness.

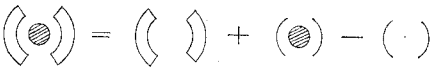

Fig. 2—Relation of the split coaxial line and its decomposite construction.

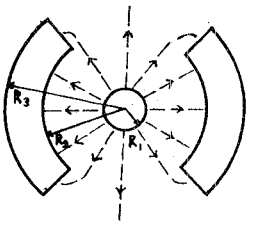

Fig. 3—Disturbance by the thick outer wall.

The curved lines in Fig. 4 show the results of the experiment using a water tank, and these are almost equal to the computed value using the approximate theory. A treatise similar to Smolarska's[3] has already been published. Our approach used almost the same transformation equation as found in treatise, but in detail, small differences are found in the papers. For example, Compare A[3] with B.[1]

1) The next formulas are adopted to transform the original figure into the orthogonal line coordinates.

   A) $\omega = \log Z$ (Transformation).

   B) $\mu = R_1 e^Z$ (Transformation).

2) The *S-C* transformation is common in both *A* and *B*, but the corresponding points differ.
   A) Corresponds with three unknown constants α, β, and γ for the singular point.
   B) Corresponds with two unknown constants α, β, for the character of the elliptic function.
3) The enumeration method of unknown constants.
   A) This uses the definite integral, namely a definite integral is used for the distance between each singular point.
   B) This uses the indefinite integral and substitutes to acquire the value of the corresponding in its consequent equation.
4) The numerical computation.
   A) The numerical computation used the approximate calculating equation as follows: $\beta \gg 1$, $\beta \gg \gamma$, and $\beta \gg \alpha$. These relations are useful only to the case of the particular split angle. However, the errors are not investigated.
   B) The approximate calculating equation is not in use and accordingly the split width is extended to the whole range.
5) The numerical compution of the characteristic impedance is calculated in the following cases.

   Line I).

   A) $R/r = 2.3, 2.6, 2.72, 3.37$.

   B) $Z_0 = 25\Omega, 50\Omega, 150\Omega$, (for the no splits).

   Line (II).

   A) $R/r = 2.72$.

   B) $Z_0 = 25\Omega, 50\Omega, 150\Omega$, (for the no splits).